SAND2000-2631C

UTILIZING COMPUTATIONAL PROBABILISTIC METHODS TO DERIVE SHOCK SPECIFICATIONS IN A NONDETERMINISTIC ENVIRONMENT

Richard V. Field, Jr.
Structural Dynamics Development
Department 9124, MS 0847
Sandia National Laboratories
Albuquerque, NM 87185-0847
rvfield@sandia.gov

John R. Red-Horse
Optimization & Uncertainty Estimation
Department 9211, MS 0847
Sandia National Laboratories
Albuquerque, NM 87185-0847
jrredho@sandia.gov

Thomas L. Paez
Validation & Uncertainty Quantification
Department 9133, MS 0557
Sandia National Laboratories
Albuquerque, NM 87185-0557
tlpaez@sandia.gov

ABSTRACT. Certain classes of engineering systems must be designed to survive operational shock environments which are difficult or impossible to describe in a comprehensive fashion. The shock response spectrum (SRS), a common measure of the severity of a shock signal, is frequently used in this situation as a standard for system qualification. Typically, the SRS is calculated by performing a series of extreme-level shock tests that are assumed to envelope the operating environment of the system. If the system can survive these tests, the SRS from each test are combined in some conservative manner to derive a single spectrum. Often, a deterministic safety factor is then applied to this composite SRS, resulting in a reference specification for design qualification. It has been shown, however, that use of the SRS in this manner can lead to an imbalance in marginal reliability. Nevertheless, this technique remains the industry's standard means of assessing system response in a shock environment. In this article, techniques utilizing computational probabilistic methods are proposed to derive a analytically-based reference SRS that prescribes a balanced level of marginal reliability. In addition, it provides a technically sound procedure for constructing design specifications in a nondeterministic shock environment. For illustrative purposes, the method is applied to a soil penetration system consisting of a nonlinear transient dynamics calculation performed on a complex finite element structural mechanics model, coupled with a spherical cavity expansion representation of the soil medium.

NOMENCLATURE

D	Soil parameter random variable
$E[\cdot]$	Operator of mathematical expectation
$f_Y(y)$	Probability Density Function (PDF) of Y
$F_Y(y)$	Cumulative Distribution Function (CDF) of Y
$g(\cdot)$	Memoryless deterministic function
M	Nondeterministic input/output map or model
n_f	Number of points in frequency vector
n_s	Number of samples used to compute PC terms
N	Number of PC terms retained in expansion
p_s, p_f	Probability that internal component survives/fails
PCE	Polynomial Chaos Expansion
r_{XY}	Correlation coefficient between r.v.'s X and Y
$\tilde{s}$	Specified marginal reliability
SRS	Shock Response Spectrum
U_i	Predicted response at ith frequency
$u_{ref}(f_i)$	Reference SRS at ith frequency
$\bar{U}$	System reliability metric
α	Angle-of-attack random variable
γ_k	kth PC coefficient of output process
Γ_k	kth multivariate Hermite polynomial
μ_X, σ_X	Mean and standard deviation of r.v. X
ξ	Standard, normal random variable
Φ	n-dimensional random vector of model parameters

1. OVERVIEW OF NONDETERMINISTIC ANALYSIS

To establish the context for the ensuing discussion, a general framework is presented for the nondeterministic analysis of a system, as depicted in Fig. 1. Here, M is an analytical model defining the map between input F and output U where in general, both M and F are nondeterministic entities. In addition, the model maps an n-dimensional parameter vector Φ, containing components that are assumed to be nondeterministic, to the response space.

When considering this problem in a probabilistic framework, all statements of interest that address the uncertainty of the output U can be written in a statistical form, $E[g(U)]$, where $E[\cdot]$ is the operator of mathematical expectation and $g(\cdot)$ is an appropriate deterministic function. With this in mind, consider

$$E[g(U)] = E_M[E_\Phi(E_F\{g(U)|M, \Phi\}|M)] . \qquad (1)$$

The three layers of conditional expectation in Eq. (1) represent the three major components needed to accurately analyze a nondeterministic system. Statements from the innermost conditional expectation are conditioned on the model and internal parameters. Hence, the calculations are performed when one model and one set of internal parameters are considered (*i.e.*, $M = m$ and $\Phi = \phi$). At this level,

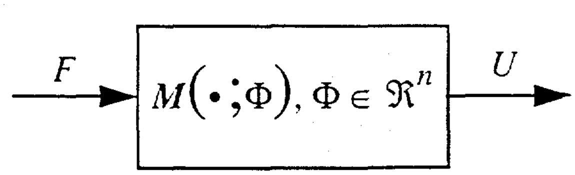

Figure 1: General framework for nondeterministic analyses.

DISCLAIMER

DISCLAIMER

statistical procedures are required only if the input F is nondeterministic. Continuing, the probabilistic character of Φ has been utilized at the second layer of Eq. (1). This is what has been commonly referred to as the "uncertainty propagation" problem; there are many computational tools to address this. It is at this level where most nondeterministic problems are solved, including the one under consideration. The third and outermost conditional expectation of Eq. (1) deals with the uncertainty in the model itself. This is a more difficult topic and is an area of continued research.

Clearly, the analysis layer, which is concerned with isolating and assessing the effects of parametric uncertainty, is a key component of a global assessment. This issue is the focus of the remaining discussion.

2. APPLICATION

A schematic of a penetration system as it impacts the ground is shown in Fig. 2, where v and γ are the velocity vector and impact angle of the system, respectively, taken to be deterministic. A considerable amount of uncertainty exists, however, in the knowledge of a particular soil parameter, D. In addition, the angle-of-attack, α, is nondeterministic due to uncertainty in the knowledge of the wind conditions. For this application, α and D were modeled as independent random variables with normal and lognormal distributions, respectively, as shown in Fig. 3. Hence, in the terminology of Eq. (1), $\Phi = \{\alpha, D\} \in \Re^2$.

The engineering question of interest is whether or not the internal component C will survive the shock environment induced by the penetration event. For historical reasons, the response measure of interest is the shock response spectrum (SRS) of the acceleration of the centroid of component C. Success, or survival, is achieved when the predicted SRS is bounded from above by a reference shock specification throughout the frequency range of interest.

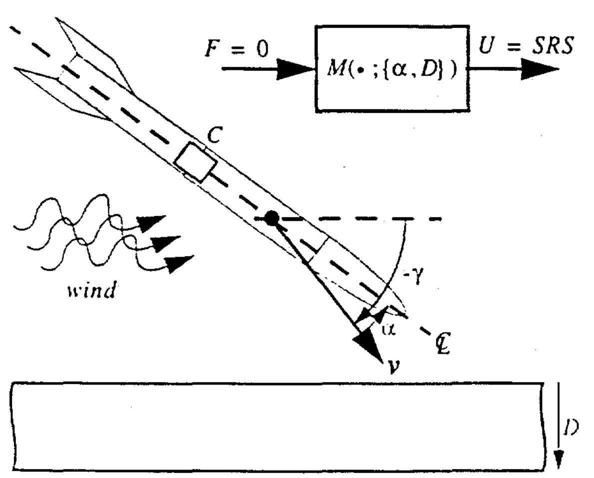

Figure 2: Problem formulation for the penetration system.

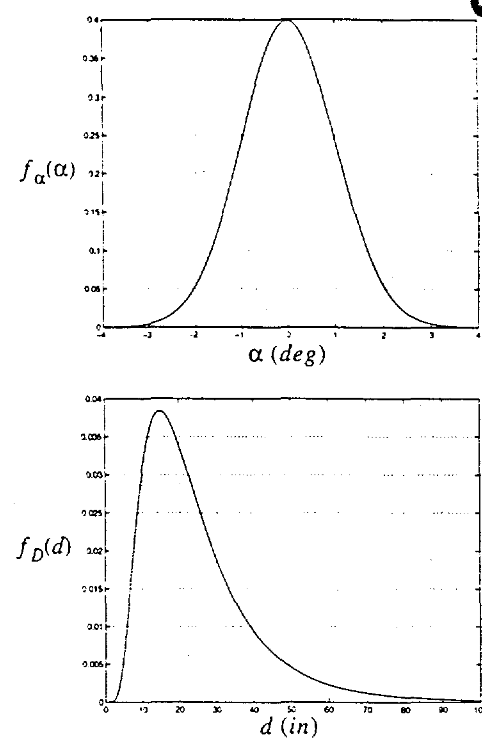

Figure 3: Density functions of random vector Φ.

As noted, this system must survive operational shock environments which are impossible to describe in a comprehensive fashion. As a result, the reference SRS referred to above is typically calculated by performing a series of extreme-level shock tests that are assumed to envelope the operating environment. If the system can survive these tests, the SRS from each test are combined in some conservative manner, then coupled with an overall safety factor, to derive a reference specification for future design qualification. It has been shown, however, that use of the SRS in this manner can lead to an imbalance in marginal reliability [5-7]. Nevertheless, it remains the industry's standard means of assessing system response in a shock environment.

PRONTO3D [2], a nonlinear, transient dynamics finite element code developed at Sandia National Laboratories, coupled with a spherical cavity expansion model of the soil-structure interaction [11], was used to calculate the predicted transient acceleration response of C during the penetration event. Filtering routines in MATLAB [10] were then used to compute the corresponding frequency-domain SRS. Each function evaluation using this complex, cascaded system model required over 33 CPU hours on a SUN Ultra II workstation. This fact motivated the use of approximations to the design space, which were developed using Box-Behnken design of experiment methods [3]. Hence, in the notation of Fig. 1, the model, M, is a polynomial response surface, quadratic in α and D, that approximates the cascaded

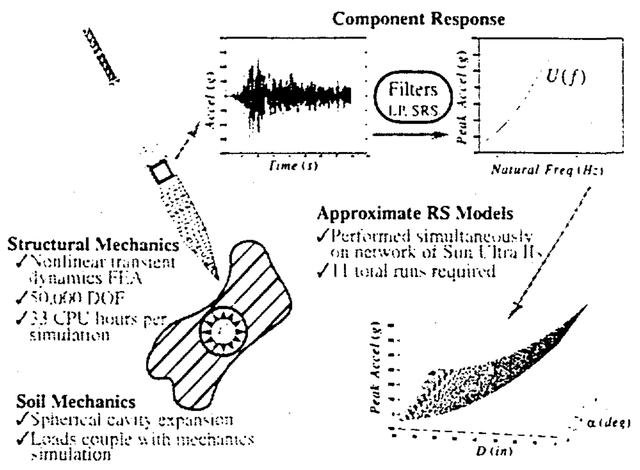

Figure 4: The model M : a complex, cascaded system.

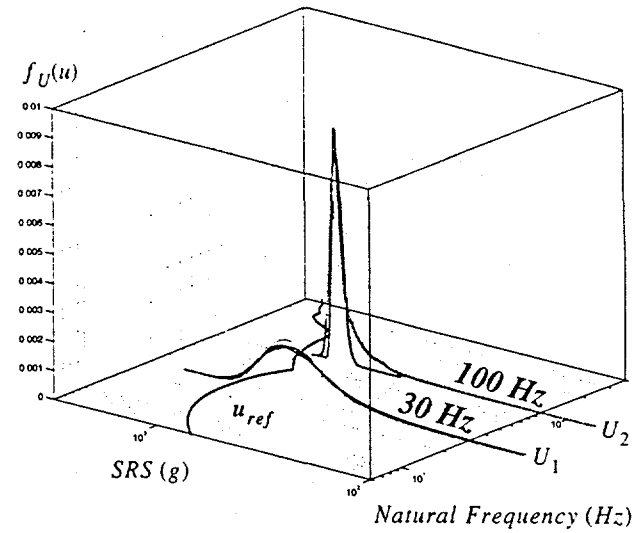

Figure 5: Frequency-wise probability of exceeding the reference SRS.

system of PRONTO3D, the cavity expansion model of the soil, and the MATLAB filtering routines. This model structure is shown graphically in Fig. 4.

3. PREVIOUS WORK

The overall goal is to estimate p_s, the probability that internal component, C, survives. In previous work [5], the authors' approach was to define a series of outputs

$$U_i = SRS(f_i),\ i = 1, 2, \ldots, n_f, \tag{2}$$

where f_i denotes the ith component of the frequency vector, discretized over n_f points. Reliability- and sampling-based methods, in conjunction with the model, $\boldsymbol{M}$, were then employed to compute corresponding marginal cumulative density functions (CDFs) $F_{U_i}(u_i)$, $i = 1, 2, \ldots, n_f$. Upon comparing to a reference, denoted u_{ref}, at each frequency line one could then make a statement regarding the probability of exceeding u_{ref}. In this regard, the frequency-wise or marginal reliability is defined to be

$$\bar{s}_i = P(U_i \le u_{ref}(f_i)) = F_{U_i}(u_{ref}(f_i)),\ i = 1, 2, \ldots, n_f. \tag{3}$$

Numerical differentiation of these marginal CDFs provide the corresponding marginal probability density functions (PDFs), two of which are illustrated in Fig. 5. The imbalance in reliability over frequency is readily apparent: at $f_1 = 30\ Hz$ there is a nonzero probability of exceeding u_{ref} (*i.e.*, $\bar{s}_1 > 0$), while at $f_2 = 100\ Hz$ the probability of exceeding the reference SRS is very small (*i.e.*, $\bar{s}_2$ is near zero). Hence, this test-based specification exhibits conservative behavior over some frequency bands, but nonconservative behavior over others. This can be partly attributed to the lack of detail present in modeling both the physical and probabilistic elements of the problem. In addition, in using this method to examine the marginal distributions of the SRS, no knowledge of the correlation between U_1 and U_2 is attained. Hence, there is no way to draw accurate conclusions regarding the probability of failure of the overall system.

As an alternative, in [6] the authors defined the scalar output

$$\bar{U} = \min_f\ (u_{ref} - U), \tag{4}$$

where U is the predicted SRS over the entire frequency band. The probability that the internal component C will not survive the penetration event can then be approximated by

$$p_f = 1 - p_s = P(\bar{U} \le 0) = F_{\bar{U}}(0). \tag{5}$$

The identical methodologies were employed under this framework to estimate $F_{\bar{U}}(\bar{u})$, and hence, p_f. Results from this approach are summarized in Fig. 6. While this methodology facilitates a system reliability assessment, the imbalance over frequency evident in Fig. 5 is concealed in the analysis.

To address the shortcomings of both of the schemes outlined above, the polynomial chaos expansion (PCE) was introduced in this framework in [7] and employed to the same application. With this framework in place, both $\bar{s}_i$, $i = 1, 2, \ldots, n_f$, and p_f can be readily computed. In addition, it can be shown that an analytically-based u_{ref} can be designed so as to specify a balanced level of marginal reliability over the frequency range of interest.

The PCE is one of the key elements of the stochastic finite element method, as developed in [9]. It relies upon the notion that random processes are mathematically well-defined mappings assumed to satisfy certain criteria. Among them is the notion that a real random variable (r.v.) is a deterministic measurable function which maps the sample space of

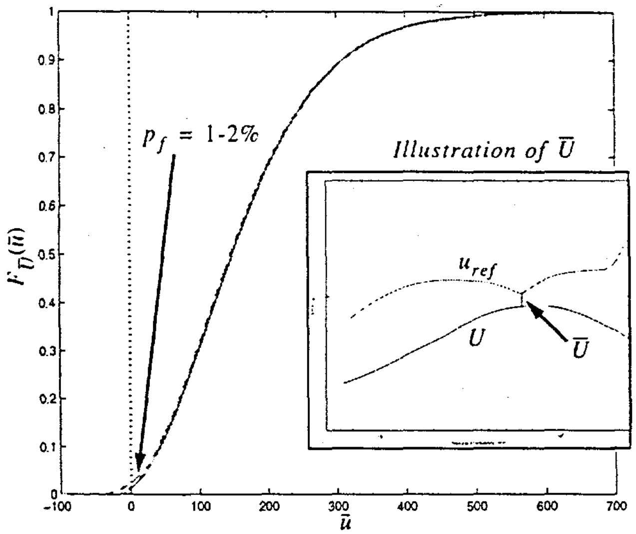

Figure 6: CDF of $\bar{U}$.

random events to the real line. It is this attribute of measurability that provides the foundation for defining a Hilbert space, $\mathcal{H}$, of square-integrable, measurable functions. This feature also establishes the foundation for a function approximation theory in $\mathcal{H}$ that directly parallels the path taken in a deterministic finite element approach with, in the stochastic case, an inner product operator that is given by mathematical expectation and the norm generated by this inner product (see [8]).

The result of this theoretical background is that finite-dimensional series approximations can be made for both the input and output random processes that can be shown to converge weakly to the functions they replace. Consider the following orthogonal decompositions, a special case of the general PCE formulation where the input and output quantities are vectors of random variables

$$\Phi(\theta) \approx \Phi(\theta)^N \equiv \sum_{k=0}^{N} \Phi_k \Gamma_k(\{\xi_l\}) \text{, and} \tag{6}$$

$$U(f, \theta) \approx U(f, \theta)^N \equiv \sum_{k=0}^{N} \gamma_k(f) \Gamma_k(\{\xi_l\}) . \tag{7}$$

Here, $\Gamma_k(\{\xi_l\})$ are defined to be multi-variate Hermite polynomials in the sequence of standard normal r.v.'s, $\{\xi_l\}$. The $\{\xi_l\}$ are defined on a sample space Ω with elements θ_l here and throughout; the explicit notation of dependence on θ is suppressed to simplify notation.

It can be shown [7] that the solutions for the Fourier coefficients in the above expansions are

$$\Phi_k = \frac{\langle \Phi \Gamma_k \rangle}{\langle \Gamma_k^2 \rangle} \text{ and } \gamma_k(f) = \frac{\langle U(f) \Gamma_k \rangle}{\langle \Gamma_k^2 \rangle} . \tag{8}$$

For this application, the expectations in Eq. (8) were approximated using a Monte Carlo scheme, where arithmetic means were substituted for the expectations

$$\Phi_k \approx \frac{\sum_{j=1}^{n_s} \Phi^{(j)} \Gamma_k^{(j)}}{\sum_{j=1}^{n_s} [\Gamma_k^{(j)}]^2} \text{ and } \gamma_k(f) \approx \frac{\sum_{j=1}^{n_s} u(f)^{(j)} \Gamma_k^{(j)}}{\sum_{j=1}^{n_s} [\Gamma_k^{(j)}]^2} , \tag{9}$$

where, $\Phi^{(j)}$, $\Gamma_k^{(j)}$ and $u(f)^{(j)}$ denote the jth out of n_s realizations of the corresponding random quantities. Computing these coefficients via Eq. (9) proves to be a rather complex process, as shown in Fig. 7. To summarize, given second order statistics $\mu_\alpha, \sigma_\alpha, \mu_D, \sigma_D, r_{\alpha D}$ and samples of two standard normal uncorrelated r.v.'s, $\{\xi_1, \xi_2\}$, the Nataf transformation from [4] can be utilized to produce samples of α and D, from which the coefficients of the expansion can be calculated. Note that to use Eq. (8) to compute the Fourier coefficients, Φ_k, one must evaluate $\Gamma_k^{(j)}(\{\xi_1, \xi_2\})$ and $\Phi^{(j)}$ with the identical sample set of $\{\xi_1, \xi_2\}$. A similar scheme is used to generate the coefficients of the response process, $\gamma_k(f)$. The sample set $\{\xi_1, \xi_2\}$ is first regenerated, but must remain fixed throughout the remaining steps. Samples of α and D can now be computed directly via Eq. (6), then passed through the model M to derive samples of the output process $U(f)$. After computing $\Gamma(\{\xi_1, \xi_2\})$ over this new sample set, Eq. (8) can be utilized to solve for the output coefficients. Again, the key issue in this process is the use of a consistent sample set of $\{\xi_1, \xi_2\}$, which is further highlighted by the dashed lines in the algorithm of Fig. 7.

Brute-force Monte Carlo sampling proves to be an inefficient means of calculating these coefficients. However, because M utilizes approximate response surface models, as illustrated in Fig. 4, computing many samples of the output $U(f)$ remains tractable. Future research will focus on more efficient methods to compute $\gamma_k(f)$, which will significantly reduce the number of function evaluations required for convergence, and

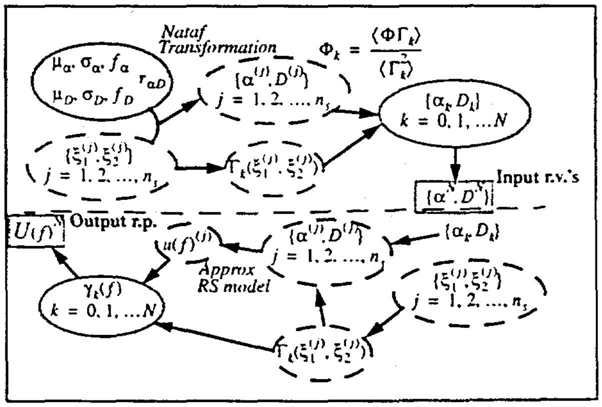

Figure 7: Algorithm used to apply the PCE.

thus allow one to bypass the need for approximate response surface models.

Once the N coefficients are computed, the expansions can be utilized to create realizations of the input and output as depicted in Figs. 8 and 9 with $N = 4$. In addition, an estimate of the correlation structure of the output random process can be computed. It is important to note that by employing the PCE technique, one arrives at an approximation to the output random process SRS, and not simply statistical information like that which is presented in Figs. 5-6. As a result, one has a more complete representation of the nondeterministic response, which can be exploited for various uses.

4. PROBABILISTIC DESIGN OF REFERENCE SHOCK

In this section, a process is developed which exploits the availability of the SRS random process to produce an analytically-based reference SRS that exhibits a prescribed level of marginal reliability at each frequency. In general, this prescribed level can be permitted to vary with frequency, allowing one to specify frequency bands where the system

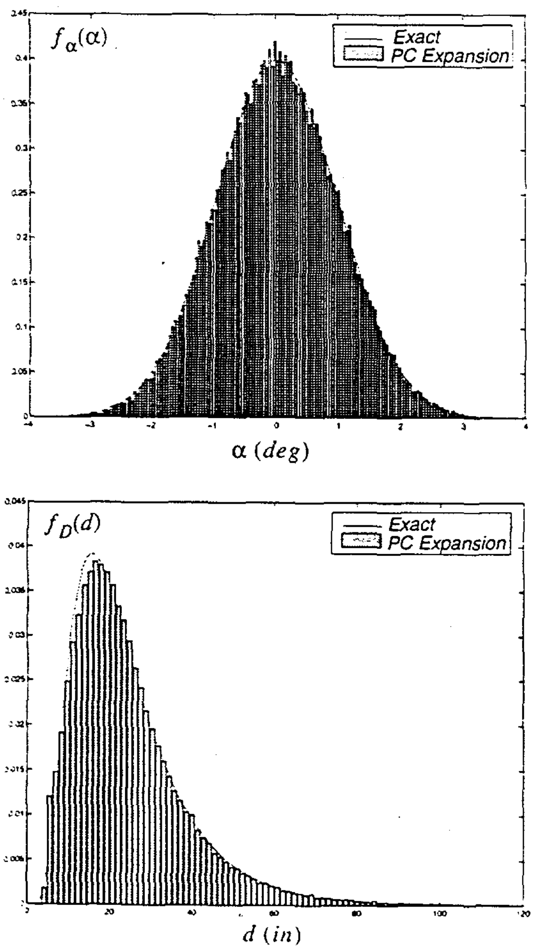

Figure 8: Density estimates of input random vector Φ using the PCE.

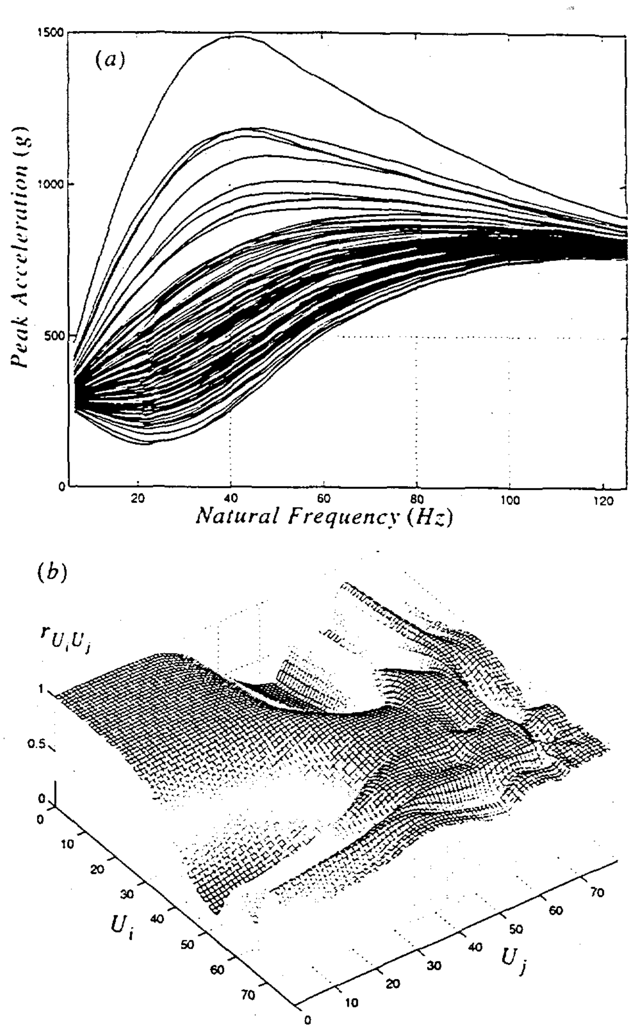

Figure 9: Polynomial chaos expansion of SRS random process: (a) 100 realizations, and (b) the estimated correlation structure.

must be more reliable, as well as frequency bands where it can be less reliable. Here, however, the marginal levels, $\bar{s}_i$, were chosen to be equal over the entire frequency range; thus ensuring a balanced marginal reliability,

$$F_{U_i}(u_{ref}(f_i)) = \bar{s}_i = \bar{s}, \; i = 1, 2, \ldots, n_f . \qquad (10)$$

To estimate the CDF of U_i at a point u_i, one can compute n_s samples of the response via the PCE expansion derived in Eq. (7), sort the realizations by magnitude, and then apply the following relation [1]

$$F_{U_i}(u_i) = \begin{cases} 0 & u_i < u_i^{(1)} \\ \frac{k}{n_s} & u_i^{(k)} \le u_i < u_i^{(k+1)} \\ 1 & u_i \ge u_i^{(n_s)} \end{cases} , \qquad (11)$$

where $u_i^{(1)}, u_i^{(2)}, \ldots, u_i^{(n_s)}$ are values of the ordered samples.

With this constant marginal reliability $\bar{s}$ specified, one can solve for the corresponding reference SRS by inverting Eq. (10)

$$u_{ref}(f_i) = F_{U_i}^{-1}(\bar{s}), \; i = 1, 2, \ldots, n_f. \qquad (12)$$

Note that Eq. (12) involves the inverse CDF of U_i, which is not explicitly known. However, by solving

$$F_i^* - F_{U_i}(\bar{s}) = 0, \qquad (13)$$

for $\bar{s}$, in conjunction with Eq. (11) via an iterative root finding method, where F_i^* is known, one can estimate $F_{U_i}^{-1}(\bar{s})$.

Once u_{ref} has been calculated, Eq. (5) can be used to estimate the probability of failure for the system. If this failure probability is unacceptable, the process must be repeated with a revised $\bar{s}$. Thus, this process can be posed as an iterative probabilistic design procedure with the following goal: for a specified target p_f, find the reference SRS that will give a marginal reliability $\bar{s}$ that is constant over frequency. The algorithm of Fig. 10 summarizes the steps required.

5. RESULTS

To illustrate this technique, assume the design specifications are such that the target probability of failure is 1 in 1000, *i.e.*, $p_f^* = 0.001$. With an initial guess of $\bar{s} = 0.999$, after five iterations of the algorithm, convergence is attained at a solution given by

$$p_f = p_f^* = 0.001, \; \bar{s} = 0.9997. \qquad (14)$$

The result of this probabilistic design is shown in Fig. 11, where it is evident that the test-based reference is nonconservative at low frequencies, but becomes conservative at 100 *Hz* and beyond. Further, as loosely illustrated by the collection of realizations shown, there is a fairly high probability of exceeding the reference SRS in the $20-80$ *Hz* range, thereby leading to a high probability of component failure.

1. Specify target probability of failure, p_f^*, and convergence tolerance ε.
2. Choose marginal reliability $\bar{s}$.
3. Solve for $u_{ref}(f_i)$, $i = 1, 2, \ldots, n_f$ via Eq. (12).
4. Solve for $\bar{U}$ via Eq. (4).
5. Evaluate p_f via Eq. (5) and compare to p_f^*.
6. Repeat steps 2-5 until $|p_f - p_f^*| < \varepsilon$.

Figure 10: Probabilistic design algorithm.

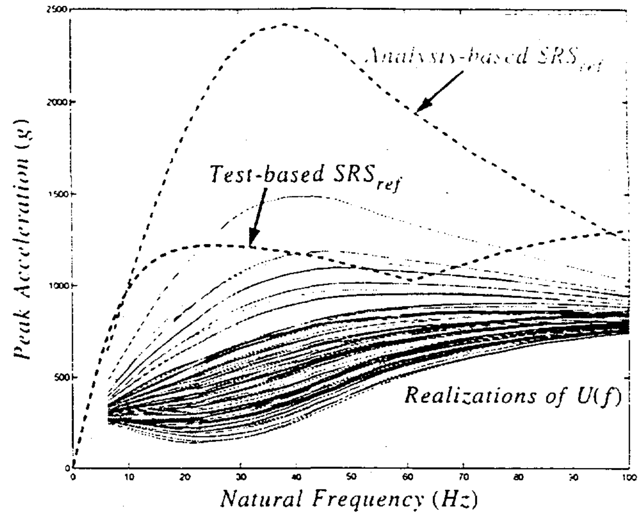

Figure 11: Analytically-based reference SRS.

This is consistent with the results presented in Figs. 5-6. In contrast, the analytically-based reference takes a shape that closely resembles the collection of realizations shown in Fig. 11. Hence, to the extent that the computational model, M, is accurate, and assuming α and D are the only significant sources of nondeterministic effects in the system, the analysis-based reference will not exhibit regions of nonconservative behavior, nor lead to overtesting of the design.

6. FUTURE WORK

Future work will focus on accelerating the convergence of the Fourier coefficients of the PCE using stratified sampling methods and various numerical integration techniques. In addition, the authors wish to address the very important issue of uncertainty in the computational model, M. Only then can the outermost layer of conditional expectation in Eq. (1) be evaluated.

7. CONCLUSIONS

One of the key elements of the Stochastic Finite Element Method, namely the polynomial chaos expansion, has been utilized in a nonlinear shock and vibration application. As a result, the computed response was expressed as a random process, which is an approximation to the true solution process, and can be thought of as a generalization to solutions given as statistics only. This approximation to the response process was then used to derive an analytically-based design specification for component shock response that guarantees a balanced level of marginal reliability. Hence, this analytically-based reference SRS might lead to an improvement over the somewhat ad hoc test-based reference in the sense that it will not exhibit regions of non conservativeness, nor lead to overtesting of the design.

8. ACKNOWLEDGEMENTS

Sandia National Laboratories is a multiprogram laboratory operated by Sandia Corporation, a Lockheed Martin Company, for the United States Department of Energy under Contract DE-ACO4-94AL85000.

REFERENCES

[1] **Ang, A.**, and **W. Tang**, *Probability Concepts in Engineering Planning and Design: Volume 1, Basic Principles*, John Wiley & Sons, Inc., New York, NY, 1975.

[2] **Attaway, S.W., K.H. Brown, F.J. Mello, M.W. Heinstein, J.W. Swegle**, J.A. Ratner, and R.I. Zadoks, "PRONTO3D User's Instructions: A Transient Dynamics Code for Nonlinear Structural Analysis", SAND98-1361, Sandia National Laboratories, Albuquerque, NM, August, 1998.

[3] **Box, G.E.P.** and **D.W. Behnken**, "Some New Three Level Designs for the Study of Quantitative Variables," *Technometrics*, Vol. 2, No. 4, 1960, pp. 455-475.

[4] **Der Kiureghian, A.** and **P. Liu**, "Structural Reliability Under Incomplete Probability Information," *Journal of Engineering Mechanics*, Vol. 112, No. 1, 1986, pp. 85-104.

[5] **Field, R.V. Jr., J.R. Red-Horse,** and **T.L. Paez**, "Reliability Analysis of Penetration Systems Using Nondeterministic Methods," *Proceedings of the 18th International Modal Analysis Conference*, San Antonio, TX, February, 2000, pp. 363-368.

[6] **Field, R.V. Jr., J.R. Red-Horse,** and **T.L. Paez**, "Nondeterministic Analysis of Shock Response Using Computational Probabilistic Methods," *Proceedings of the 14th ASCE Engineering Mechanics Conference*, Austin, TX, May, 2000, CD proceedings.

[7] **Field, R.V. Jr., J.R. Red-Horse,** and **T.L. Paez**, "A Nondeterministic Shock and Vibration Application Using Polynomial Chaos Expansions," *Proceedings of the ASCE Joint Specialty Conference on Probabilistic Mechanics and Structural Reliability*, Notre Dame, IN, July, 2000, CD proceedings.

[8] **Friedman, A.**, *Foundations of Modern Analysis*, Dover Publications, Inc., New York, NY, 1982.

[9] **Ghanem, R.G.** and **P.D. Spanos**, *Stochastic Finite Elements: A Spectral Approach*, Springer-Verlag, New York, NY, 1991.

[10] *MATLAB User's Guide*, The MathWorks, Inc., Natick, MA, 1998.

[11] **Warren, T.L.** and **M.R. Tabbara**, "Spherical Cavity Expansion Forcing Function in PRONTO3D for Application to Penetration Problems," SAND97-1174, Sandia National Laboratories, Albuquerque, NM, May, 1997.